ICM11

Modeling the growth of LT and TL-oriented fatigue cracks in longitudinally and transversely pre-strained Al 2524-T3 alloy

L.P. Maduro[a], C.A.R.P. Baptista[a]*, M.A.S. Torres[b], R.C. Souza[c]

[a]Escola de Engenharia de Lorena, EEL/USP, Department of Materials Engineering, Lorena,SP Cx. Postal 116, CEP 12602-810, , Brazil
[b]Universidade Estadual Paulista, FEG, Department of Mechanics, Guaratinguetá,SP, CEP 12516-410, Brazil
[c]Instituto Federal de São Paulo, Campus São João da Boa Vista, IFSP/SJBV, Jardim Itália, SJBV, SP, CEP 13872-551, Brazil

Abstract

The aluminum alloy 2524 (Al-Cu-Mg) was developed during the 90s mainly to be employed in aircraft fuselage panels, replacing the standard Al 2024. In the present analysis the fatigue crack growth (FCG) behavior of 2524-T3 was investigated, regarding the influence of three parameters: load ratio, pre strain and crack plane orientation of the material. The pre strain of aluminum alloys is usually performed in order to obtain a more homogeneous precipitates distribution, accompanied by an increase in the yield strength. In this work, it was evaluated the resistance of Al 2524-T3 sheet samples to the fatigue crack growth, having L-T and T-L crack orientations. FCG tests were performed under constant amplitude loading at three distinct positive load ratios. The three material conditions were tested: "as received"(AR), pre strained longitudinally (SL) and transversally (ST) in relation to rolling direction. In order to describe FCG behavior, two-parameter kinetic equations were compared: a Paris-type potential model and a new exponential equation introduced in a previous work conducted by our research group. It was observed that the exponential model, which takes into account the deviations from linearity presented by da/dN versus ΔK data, describes more adequately the FCG behavior of Al 224-T3 in relation to load ratio, pre strain effects and crack plane orientation.

© 2011 Published by Elsevier Ltd. Selection and peer-review under responsibility of ICM11

Keywords: aluminum alloys; pre strain; fatigue crack growth; modeling

1. Introduction

Aluminum alloys have been the most widely used structural materials in aircraft industry due to their favorable strength-to-weight ratio. Among aluminum alloys of the 2XXX series (Al-Cu-Mg), the most known and employed is Al2024. Efforts to decrease the impurities (iron and silicon) content lead to the improved Al 2524 T3 alloy. This alloy was developed by ALCOA to be used in the Boeing 777 Project, replacing the standard Al 2024. Its more rigorous processing control provides approximately 15-20% improvement in fracture toughness, twice the fatigue crack growth (FCG) resistance [1] and 30-40% longer time to failure [2] when compared with 2024, without loss of strength or corrosion resistance [3,4].

Pre strained aluminum alloys usually show a more homogeneous precipitates distribution, which should increase the yield strength. Since these alloys are susceptible to fatigue crack growth during their application, it is important to evaluate the pre strain effects on crack growth behavior, at different crack plane orientations and load conditions. In relation to the influence of the pre straining on FCG behavior, some data from Al 7475-T7351 and Al 7050-T7451 alloys are available [5,6]. However, no information on the effects of the pre straining on FCG behavior of Al 2524 T3 was found in literature.

To account for the FCG behavior, fracture mechanics based models have been largely employed. The first FCG model relating the fatigue crack growth rate (da/dN) with the stress intensity range (ΔK), was proposed by Paris and Erdogan [7]. This approach became the canonic model even though it does not consider the effects of the stress ratio (R) on the crack propagation. In order to explain the R effects, Elber [8] introduced the concept of crack closure and the effective stress intensity factor range

---

(ΔKeff). However, the various difficulties inherent to closure measurements lead to the search of alternative methods to take into account the stress cycle asymmetry. Sadananda and Vasudevan [9], in their Unified Approach, have proposed that the FCG rate should be described by two driving forces, ΔK and Kmax, ignoring the closure measurements. Although several two-parameter models have been previously developed, none of them assume the existence of two independent driving forces for crack growth [10,11,12].A potential bi-parametric model, proposed in previous works [13,14] by our research group, see equation (1), assumes the exponents of ΔK and Kmax as independent, being capable of predicting the FCG behavior under experimental conditions differently from those employed in calculating its constants. All of the conventional Paris-based models are represented by a straight line in a log-log plot, for a fixed R value. However, some metals and alloys do not have a high degree of linearity in the region of intermediate crack growth rates. For example, the real fatigue data of aluminum and titanium alloys can show several knees or transitions, which are changes in the slope of the da/dN-ΔK plots [15,16]. In order to account for this non-linear behavior, a new exponential model, see equation (2), was proposed in a previous work [17].

$$\frac{da}{dN} = C(\Delta K)^f (K_{\max})^g \qquad (1)$$

where C, f and g are the fitting coefficients.

$$\frac{da}{dN} = Ae^{\frac{\beta}{\Delta K}} \text{, where } A = e^{\alpha} \qquad (2)$$

where α and β are the fitting coefficients.

The purpose of the present work is to analyze the FCG behavior of 2524-T3 aluminum alloy regarding the influence of stress ratio, pre-strain of the material and crack plane orientation (L-T and T-L). Bi-parametric potential and exponential modeling is employed in the description of the R-effects.

2. Material and experimental procedure

Aluminum alloy sheets of 2524-T3 with thickness of 2.5 mm were employed in this work. Three distinct material conditions were tested: "as received" (AR), pre strained longitudinally (SL) and transversally (ST) in relation to the rolling direction. The material was pre strained by stretching the original sheets from their extremities to a thickness reduction level of 20%, usually adopted by the aircraft industry. Hence, the AR and SL thicknesses are 2.0mm. The chemical composition is shown in Table 1.From the original and pre strained sheets, tensile test specimens were cut in longitudinal and transversal directions, according to ASTM E8 [19]. The M(T) specimens adopted for FCG tests were cut in L-T and T-L directions, according to ASTM E647 [20].Center-cracked M(T) specimens, cut in the L-T and T-L orientations, were adopted for this work. FCG tests were performed in a MTS servo hydraulic testing machine under constant amplitude loading at different positive stress ratios, R=0.1, 0.3 and 0.5. All tests were conducted at a constant frequency of 10 Hz and the loading waveform was sinusoidal. The crack length was measured using the compliance method. All of the experimental procedures were in conformity with ASTM E647 standard [20].

3. Results and discussion

3.1. Microstructural Characterization

Figure 1 shows the microstructure of the three material conditions, longitudinally oriented to rolling direction. The average grain dimensions of the AR condition (fig1a) are the following: 96±17μm in length, 22±2μm in height and 74±9μm in width. The average grain dimensions of the SL condition (fig1b) are the following: 111±13μm in length, 20±2μm in height and 96±17μm in width. The average grain dimensions of the ST condition (Fig 1c) are the following: 105±17μm in length, 18±1μm in height and 108±14μm in width. By comparing the grain dimensions, slight increases were observed in the pre strained conditions as compared to the AR material. Fine microstructural features were revealed for the AR condition by scanning electron microscopy (SEM) as shown in Figure 1d. In this figure, the white particles are intermetallic compounds which appeared during the precipitation hardening process. Also in Figure 1d, the dark region is the clad, a very thin aluminum superficial coat (approximately 100μm), applied to improve the corrosion resistance. The largest second phase medium size is about 5μm. Second phase particles smaller than 1μm were also observed. EDS (Energy dispersive spectrography) analyses revealed that the clad is composed of approximately 93% Al.
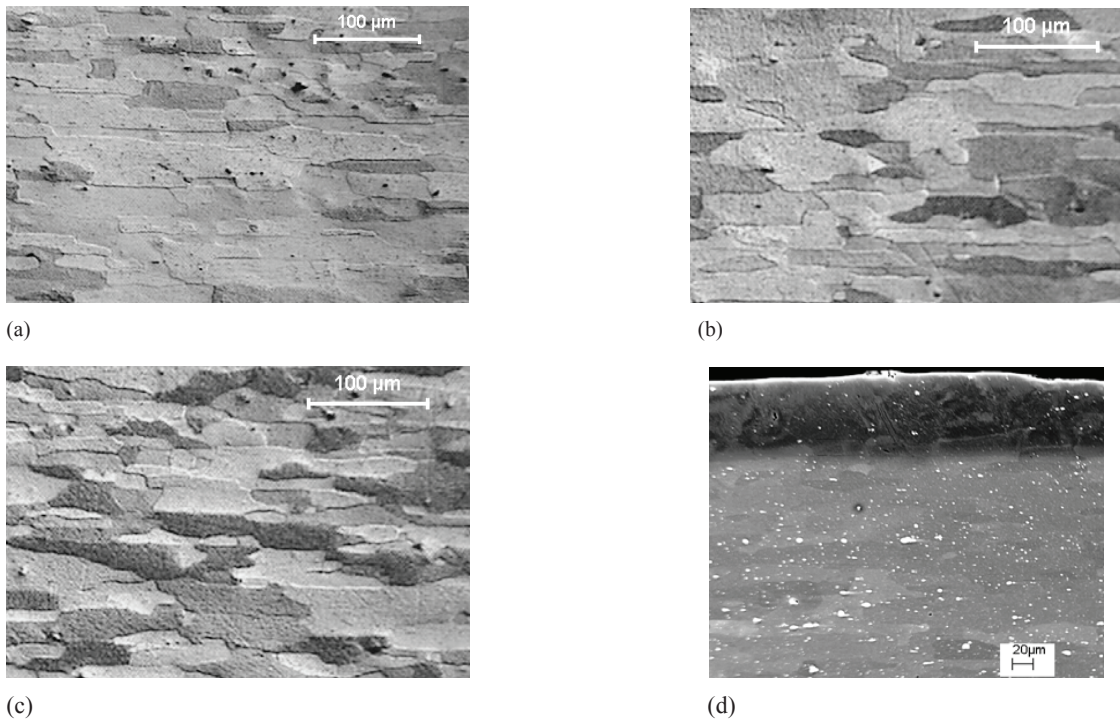
(a)

(b)

(c)

(d)

Fig. 1: As received Al 2524-T3 optical micrograph, longitudinal orientation, for: (a)AR; (b) SL; (c) ST material conditions; (d) SEM micrograph for AR condition showing the clad (dark region), matrix and the distribution of the second phase particles (white particles)

3.2. Tensile test

The results (average of three tests for each of the studied conditions) are presented in Table 1. The yield stress increases with the pre strain for both conditions (SL and ST). The strain hardening exponent and the total strain are smaller for the pre strained conditions. These results are associated with the hardening effects occurred during the pre straining process.

Table 1: Room temperature tensile test properties of Al2524-T3 alloy. σ_{YS}, yield stress; σ_{TS}, ultimate tensile strength; E, Young's Modulus; ε total strain; k and n, strain hardening parameters.

Mechanical Properties of Al2524-T3						
Direction	Condition	σ_{YS} (MPa)	σ_{TS} (MPa)	n	k-	ε (%)
longitudinal	AR	320	436	0.16	680	17
	ST	325	439	014	657	14
	SL	360	440	0.12	633	13
transversal	AR	292	428	0.17	675	18
	ST	317	417	0.14	624	19
	SL	306	420	0.14	638	16

3.3. Fatigue crack growth analysis

The experimental points, da/dN versus nominal ΔK, for all material conditions (AR, SL and ST) are plotted in Figure 2 for L-T and for T-L crack orientation, both in a log-log scale for the three adopted R-ratios.In these figures it can be seen that the FCG points that referred to each R-ratio have a similar behavior for all the material conditions. For a given ΔK, the crack growth rate da/dN is increased as R increases. Thus, the pre-straining has no significant influence in the FCG behavior for both crack plane orientations. This behavior is in accordance to the low variation in grain size resulting from the pre straining process (see item 3.1) despite any residual stress that may have been induced.

Figure 3 shows the experimental points for AR condition comparing the behavior of LT and TL crack orientations. It can be seen that cracks with TL orientation have larger propagation rates than LT cracks for a given load ratio. This result was also observed for pre strained conditions (SL and ST), indicating that the cracks were more likely to propagate along the grain length direction than in the grain width direction. A close analysis of the periodic deflections observed in crack path identified a higher number of deflections for TL-oriented cracks which presented a higher ability to disengage themselves from microstructural obstacles (grain boundaries, hard particles) when compared to the LT cracks for all the material conditions (Table 2 and Figure 4a).

The fatigue crack propagation resulted in plane fracture surfaces, showing shear lips occupying higher portions of the thickness as the cracks became longer. SEM fractographs revealed that the fracture mechanisms were similar for all the materials conditions. Besides the ductile fatigue striations, large intermetallic particles could also be seen. Figure 4b shows one of these particles, with approximately 10 μm in size, involved by fatigue striations. It can be observed that the crack deviated from the particle, which was not broken.
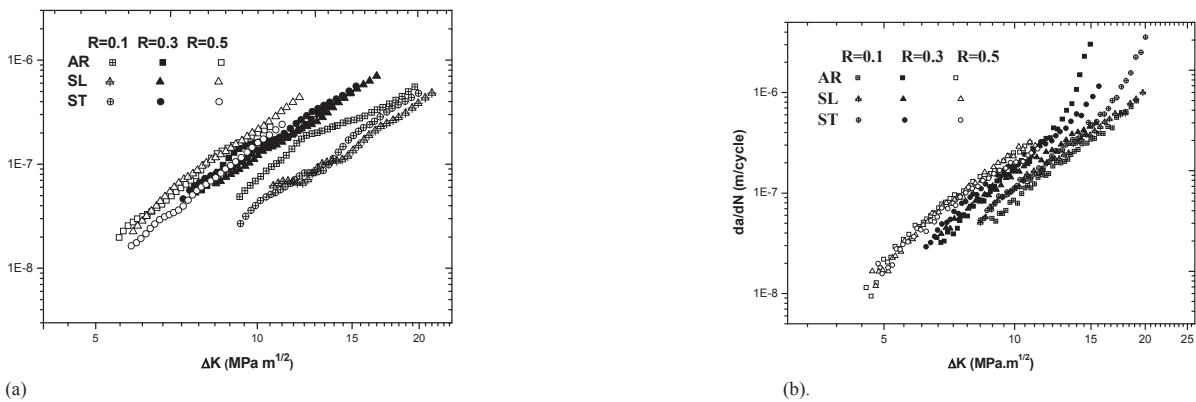

(a)

(b).

Fig. 2: FCG experimental results of Al2524-T3, corresponding to various R (stress ratio) values, for the three conditions (AR, ST and SL) (a) L-T crack orientation; (b) T-L crack orientation.
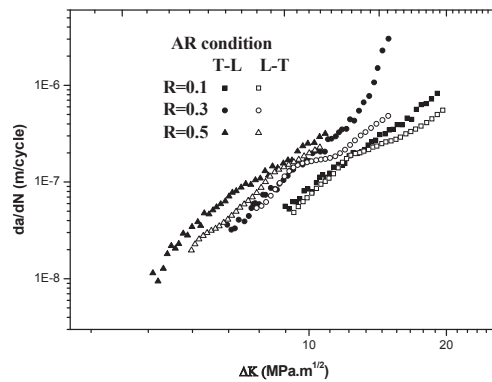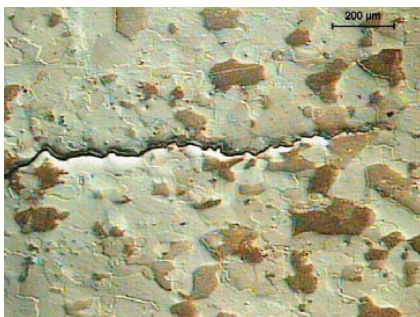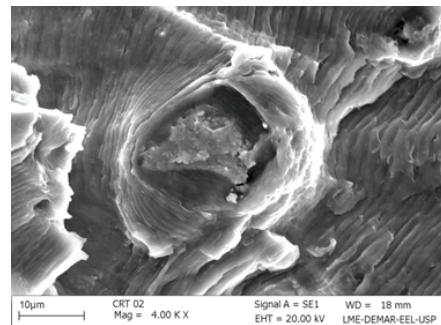

Fig. 3. FCG experimental points for AR condition, L-T and T-L crack orientations.

(a)

(b)

Fig. 4. (a) Crack path for AR condition 100x (b) SEM fractograph of sample tested with R = 0.3, for AR condition and T-L crack orientations

Table 2. Number of deflections in crack path

Material condition	CR		SL		ST	
Crack orientations	LT	TL	LT	TL	LT	TL
Number of deflections	2.5	2.8	2.1	2.8	2.3	2.5

3.4. FCG rate modeling

An exponential bi-parametric model, represented by equation (3) and developed by our research group [21] is compared to the bi-parametric potential model given by equation (1). This model describes FCG for a given material in function of two independent loading parameters, ΔK and R, being capable of more accurately describing the common deviations of linearity observed in experimental data.

$$\frac{da}{dN} = e^{\alpha} e^{\frac{\delta \log(R) + \gamma}{\Delta K}} \qquad (3)$$

In order to calculate the model coefficients α, δ and γ, a new parameter Y is defined by equation (4). The same algorithm was used in order to calculate the fitting coefficients of both bi-parametric models, the potential, see equation (1), and the exponential, given by equation (3).

$$Y = \alpha \Delta K + \delta \log(R) + \gamma \qquad (4)$$

The coefficients α, δ and γ were calculated and the curves reconstitutions were performed for the three material conditions (AR, SL and ST). Figure 5a shows the curves generated by bi-parametric exponential model for the SL condition and LT crack orientation. Figure 5b shows the results obtained by the bi-parametric potential model for the same experimental condition

(a)   (b)
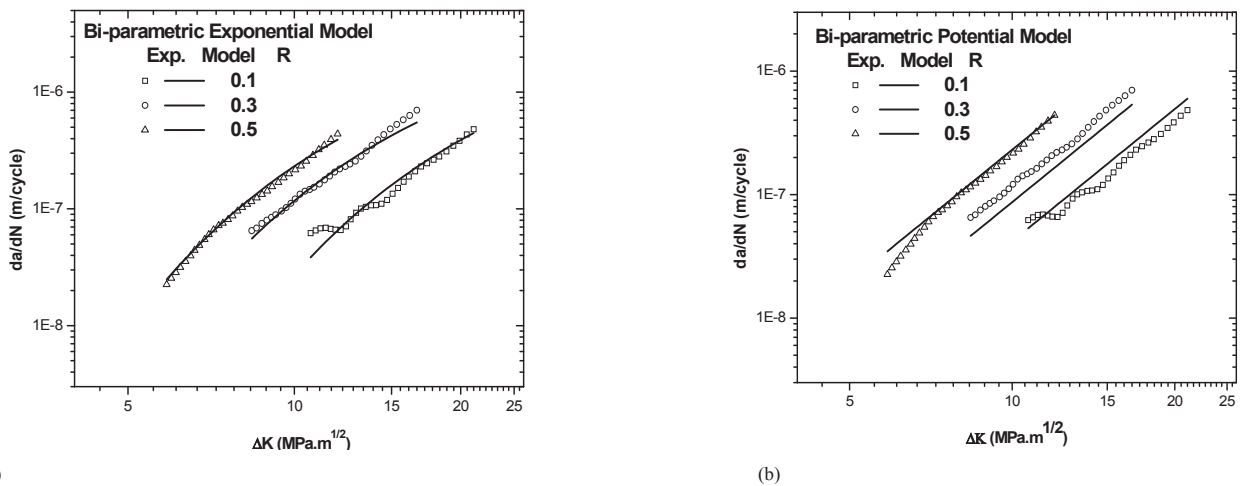
Fig. 5: FCG curves of SL condition and L-T orientation, described by (a) bi-parametric exponential model. (b) bi-parametric potential model.

A visual examination of the curves shown in Fig. 5 reveals that the exponential model provides a better fit to the FCG data when compared with the potential model. The accuracy of these models is evaluated by using the criterion of normalized sum of residuals, as shown in equation 5 where p is the number of points in each curve and "exp" and "mod" subscripts refer to experimental and model points, respectively. The results for all material conditions and crack orientations are presented in Table 3. It can be seen that the exponential model shows lower residuals for all of the material conditions and crack orientations, which means that this equation gives a better description of the FCG behavior of the material.

$$Er = \sum_{i=1}^{p} \sqrt{\left(\frac{da/dN_{\exp} - da/dN_{\mathrm{mod}}}{da/dN_{\exp}}\right)^2} \Bigg/ p \qquad (5)$$

Table 3: Normalized sum of residuals for L-T orientation and T-L orientation

		L-T orientation			T-L orientation		
Model	Condition	R=0.1	R=0.3	R=0.5	R=0.1	R=0.3	R=0.5
Exponential	AR	0.0064	0.0134	0.0052	0.0065	0.0167	0.0445
	SL	0.0246	0.0081	0.0048	0.0068	0.0250	0.0208
	ST	0.0270	0.0629	0.0717	0.0134	0.0109	0.0531
Potential	AR	0.0354	0.0380	0.0311	0.0103	0.0276	0.0137
	SL	0.0380	0.0593	0.0328	0.0085	0.0761	0.2795
	ST	0.0984	0.1464	0.0788	0.0535	0.1259	1.9271

4. Conclusions

The experimental results presented in this work demonstrated that the pre-straining of 2524 T3 aluminum alloy has no significant influence in the FCG behavior for both TL and LT-oriented cracks. This behavior is in accordance to the low variation in grain size resulting from the pre straining process. It was also observed that TL cracks in 2524-T3 aluminum alloy sheet propagate faster than LT cracks for all of the studied material conditions. The exponential bi-parametric model presented in this work was found to be adequate to model the FCG behavior of the material in the AR and pre-strained conditions.

References

[1] Williams JC., Starke Jr EA. Progress in structural materials for aerospace systems. *Acta Mater* 2003;19: 5775-99.

[2] Golden PJ, Grandt Jr AF, Bray GH. A comparison of fatigue crack formation at holes in 2024-T3 and 2524-T3 aluminum alloy specimens. *International Journal of Fatigue* 1999;21:211-219.

[3] Imarigeon JP, Holt RT, Koul AK, Zhao L, Wallace W, Beddoes JC. Lightweight materials for aircraft applications. *Mater Charact* 1997;35:41-67

[4] Satarke Jr EA, Staley JT. Application of modern aluminum alloys to aircraft. *Prog Aerospace Sci* 1996;32:131-172

[5] Al-Rubaie KS, Barroso EKL, Godefroid LB. Fatigue crack growth analysis of pre strained 7475-T7351 aluminum alloy. *International Journal of Fatigue* 2006;28:129-139.

[6] Al-Rubaie KS, Del Grande MA, Travessa DN, Cardoso KR. Effect of the pre strain on fatigue life of 7050-T7451. *Material Science and Engineering* 2007;464:141-150.

[7] Paris P, Erdogan F. A critical analysis of crack propagation laws. *J. Basic Engng, Trans. ASME* 1963;528-534.

[8] Elber W. The significance of fatigue crack closure. In: Damage Tolerance in aircraft structures. *ASTM STP 486*, Philadelphia, USA, 1971, p.230-247.

[9] Sadananda K.; Vasudevan AK. Unified approach to fatigue crack growth. In: *ICM 8, International Conference on Mechanical Behavior of Materials*, 1999, Victoria, Canada. *Proceedings,* V.1.6, .283-288.

[10] Walker K. The effect of stress ratio during crack propagation and fatigue for 2024-T3 and 7075-T6 aluminum. In: Effects of Environmental and Complex Loading History on Fatigue Life, *ASTM STP 462*, Philadelphia, USA, 1970, p.1-14.

[11] Kujawski D. A new $(\Delta K^+K_{max})^{0.5}$ driving force parameter for crack growth in aluminum alloys. *International Journal of Fatigue 2001;*23:733-740.

[12] Forman RG, Kearney VE, Engle RM. Numerical analysis of crack propagation in cyclic-loaded structures. *J. Basic Eng., Trans. AIME*: 1967; 459-464

[13] Baptista CARP.; Torres MAS, Patoukhov VA, Adib AML. Development and evaluation of two-parameter models of fatigue crack growth. In: International Fatigue Congress, 9., 2006, Atlanta. *Proceedings*… Oxford: Elsevier, 2006. 1 CD-ROM.

[14] Adib AML, Baptista CARP., Pastoukhov VA., Torres MAS. Describing the cycle asymmetry effects on fatigue crack growth with a bi-parametric exponential equation., In: *International Congress of Mechanical Engineering*, 2007.

[15] Swain MH, Everett RA., Newman Jr JC., Philips EP. In: Edwasrds PR, Newman Jr, JC. (Eds.). Short Crack Growth Behavior in Various Aircraft Materials*, AGARD.***,** R-767, 1990, p. 7.1-7.30.

[16] Ishii H, Choi SJ, Tohgo K. International Conference on Mechanical Behavior of Materials, ICM8, Victoria, Canada, 1999, *Proceedings,* V.I.2, p.73-78.

[17] Adib AML, Baptista CARP. An exponential equation of fatigue crack growth in titanium, *Materials Science and Engineering* 2007;452-453:321-325.

[18] Sadananda K, Vasudevan AK. Crack tip driving forces and crack growth representation under fatigue. *International Journal of Fatigue* 2004;26:39-47.

[19] ASTM E8. *Standard test methods for tension testing of metallic materials.* Annual book of ASTM standards, ASTM; 2001

[20] ASTM E647**.** *Standard test method for measurement of fatigue crack growth rates.* Annual book of ASTM standards. ASTM; 2001.

[21] Adib AML. *Estudo da propagação de trincas por fadiga em carregamentos de amplitude constante: um novo modelo cinético.* Master Dissertation, EEL/USP, Lorena, Brazil, 2006. (in portuguese)